sustainability

MDPI

Article

Integral Recovery of Almond Bagasse through Dehydration: Physico-Chemical and Technological Properties and Hot Air-Drying Modelling

Stevens Duarte, Ester Betoret, Cristina Barrera, Lucía Seguí and Noelia Betoret *

Instituto Universitario de Ingeniería de Alimentos para el Desarrollo, Universitat Politècnica de València, 46022 Valencia, Spain; steduase@doctor.upv.es (S.D.); mesbeval@upvnet.upv.es (E.B.); mcbarpu@tal.upv.es (C.B.); lusegil@upvnet.upv.es (L.S.)

* Correspondence: noebeval@tal.upv.es; Tel.: +34-963877000 (ext. 73658)

Abstract: Recovering waste from industrial food processes and developing new healthy foods as plant protein sources has been a major focus of scientific research and industrial innovation in food. Thus, the consumption of plant-based beverages from soy, oat, or almond has been promoted. In the case of almonds, the resulting solid bagasse has an interesting nutritional profile and its transformation into a powdered product could be a valuable option for the food industry. The main objective of this work was to determine the effect of hot air drying at 60 and 70 °C and freeze-drying on the physicochemical, water interaction, emulsifying and antioxidant properties of powdered almond bagasse. Furthermore, hot air-drying curves have been modelled and isotherms at 20 °C have been performed. The proximate composition of the powder revealed a protein content of 15% and a fat content of 25%, which makes it a remarkably different powder from those obtained from other vegetable residues such as fruits and vegetables. This composition was decisive in the effect of the drying method and drying temperature, and no significant differences were observed on the physico-chemical or antioxidant properties regardless of the drying method used. However, freeze-drying resulted in a powder with a more homogeneous particle size distribution and better oil-interaction properties, especially with higher emulsifying activity and stability.

Keywords: plant-based almond drink; almond; solid bagasse; air drying; freeze drying; sorption isotherms

Citation: Duarte, S.; Betoret, E.; Barrera, C.; Seguí, L.; Betoret, N. Integral Recovery of Almond Bagasse through Dehydration: Physico-Chemical and Technological Properties and Hot Air-Drying Modelling. *Sustainability* **2023**, *15*, 10704. https://doi.org/10.3390/su151310704

Academic Editors: Ping Dong and Long Yu

Received: 6 June 2023
Revised: 27 June 2023
Accepted: 4 July 2023
Published: 7 July 2023

1. Introduction

The food industry has become increasingly aware of the impact of food waste in economics and environment, and the need to reduce it. In fact, primarily motivated by the fulfilment of the Sustainable Development Goals (SDG), 71% of Spanish companies have a defined internal strategy to fight against food waste [1]. The production of new functional ingredients, biofuel production, or bioactive compounds extraction are some of the most considered strategies for food processing residues valorization [2–4]. The composition profile of the residues and their physico-chemical properties must be known in order to identify the opportunity for revalorization and to determine the possible uses [5].

The new trends in food development have been defined in the last years by the increased consumer awareness for health and sustainability and the growing incidence in allergies or food intolerances. Thus, the consumption of plant-based food has been promoted. Plant-based beverages or vegetable drinks are a clear example of this new orientation; more weight is being put behind them as an alternative to the consumption of dairy drinks. Among these, vegetable drinks such as soy, oats, rice, almond, and coconut stand out. In the manufacturing process, the raw material is soaked in water, milled, and filtered, resulting in a liquid phase that will constitute the vegetable beverage. The

remaining solid material is usually referred to as press cake or bagasse, and it is usually discarded or used for animal feed or as fertilizer [6].

Regarding the almond, a relevant area is dedicated to its cultivation in Spain, only behind the olive and the grape [7]. Its consumption as a nut is growing due to the healthy properties associated with its unsaturated fatty acids (56%), proteins (23%), fiber (11%) and other carbohydrates (7%), minerals, and vitamins content [8]. Additionally, and motivated by new consumer trends, it is being increasingly used as the raw material for obtaining vegetable almond drink. The resulting solid bagasse has an interesting nutritional profile, which makes it very attractive for valorization. Its transformation into a powdered product with good nutritional properties for use as a functional food ingredient could be an option [9,10]. Determining its physico-chemical, technological, and functional properties is essential in determining its best use.

The main objective of this study was to determine the effect of hot air-drying at 60 and 70 °C and freeze-drying on the physico-chemical, water interaction, emulsifying, and antioxidant properties of powdered almond bagasse. Furthermore, hot air-drying curves have been modelled and isotherms at 20 °C have been performed.

2. Materials and Methods

2.1. Process for Obtaining Almond Bagasse and Almond Bagasse Powder

Natural peeled almonds were purchased from a local supermarket and ground with tap water in a ratio of 1/9 (*w/w*). A domestic food processor (Thermomix®, Vorwerk, Spain) at 10,000 rpm for 20 s was used. The grind was then filtered with a stainless steel 500 µm sieve and the almond bagasse was recovered for further characterization and processing. The recovered bagasse mass was about 82% of the rehydrated kernel mass.

For obtaining the dried almond bagasse, the moist almond bagasse was distributed homogeneously in plastic grids with a nominal opening of 2 mm and then introduced into the dryer until a water activity (a_w) below 0.3 was reached. A convective dryer (Pol-eko Aparatura, Katowice, Poland) with cross-flow air at a velocity of 10 m/s at 60 or 70 °C for 10 h and 7 h, respectively, was used to obtain air dried (HAD) bagasse, and a freeze-dryer (Telstar, Lioalta-g) was used to obtain the freeze-dried (LYO) one from almond bagasse previously frozen at −40 °C for 24 h. The inlet air to the convective dryer was ambient air at 25 °C and 25% of relative humidity. After that, the dried almond bagasse was ground using a food processor (Thermomix®, Vorwerk, Spain) at 4000 rpm for 20 s in intervals of 5 s and then at 10,000 rpm for 20 s in intervals of 5 s, thus obtaining almond bagasse powders with coarse granulometry. Finally, the powders were stored at 20 °C in light-opaque glass jars to prevent deterioration and oxidation reactions.

During the hot air-drying experiments, the samples weight change was registered. The evolution of the moisture content was determined from the initial moisture content and the mass of the samples at each time. Plotting the moisture on dry basis versus time made it possible to graph the drying curves and, from these, the drying rate curves. Data were modeled according to a lineal empirical and diffusional models. The goodness of fit was assessed by the coefficient of determination (R^2) (Equation (1)), the root mean square error (RMSE) (Equation (2)), and the mean relative error (MRE) (Equation (3)). For the best fit, the R^2 should be high and RMSE and MRE should be low.

$$R^2 = 1 - \frac{\sum_{i=1}^{n}\left(x_{exp,\,i} - x_{pred,\,i}\right)^2}{\sum_{i=1}^{n}\left(x_{exp,\,i} - \overline{x}\right)^2} \quad (1)$$

$$RMSE = \frac{\sqrt{\sum_{i=1}^{N}\left(x_{exp,\,i} - x_{pred,\,i}\right)^2}}{N} \quad (2)$$

$$\mathrm{MRE} = \frac{1}{\mathrm{N}} \sum_{\mathrm{i}=1}^{\mathrm{N}} \frac{\left| x_{exp,\,i} - x_{pred,\,i} \right|}{x_{exp,\,i}} \quad (3)$$

where x represents the variable under consideration, i.e., the velocity in the linear model and the reduced driving force in the diffusional model; $\overline{x}$: represents the mean value; N is the number of determinations; *exp.*; experimental. *pred*: predicted by the model.

2.2. Analytical Determinations

The water activity (a_w) of almond bagasse and almond bagasse powders (air dried at 60 °C and 70 °C and freeze-dried) was determined with a dew point hygrometer (DECAGÓN Aqualab 4TE) at 20 °C. The moisture content was determined following the official method in dried fruits established by the AOAC [11]. The total soluble solids (TSS) were determined by refractometry. For this, a dilution of the sample in distilled water was carried out in a ratio of 1:10 (m/v) and the Brix degrees were measured by means of a refractometer (ABBE ATAGO 3-T) thermostated at 20 °C. The fat content of almond bagasse was determined by Soxhlet extraction with petroleum ether according to the method established by the AOAC [12]. A relation of 5 g sample/90 mL solvent at 290 °C was used. The protein content was determined by the Kjeldahl method, considering 5.18 as the conversion factor from N to protein [13]. Different Van Soest fiber fractions, including neutral detergent fiber, which corresponds to the lignin, cellulose, and hemicellulose contents (NDF), acid detergent fiber, which corresponds to the lignin and cellulose contents (ADF), and lignin with acid detergent, which corresponds to the pure lignin content (LDF), were determined [14]. The values were used to estimate hemicellulose, cellulose, and lignin content. The ash determination was carried out by incineration of the material in a muffle at 550 °C [15].

Water Interaction and Emulsifying Properties

The solubility (SD) was determined following the procedure described by Mimouni et al. [16], in which the mass fraction of a dissolved solid (SS) in a rehydrated sample (TS) is determined. The hygroscopicity was evaluated according to the method described by Cai and Corke [17]; 0.5 g of each sample was weighed in glass crucibles and taken to an airtight chamber next to a saturated solution of sodium sulfate (Na_2SO_4) for 7 days at 25 °C. Wettability, defined by the time it takes for a sample to become wet in its entirety, was determined by weighing 2 g of each powder sample slowly poured into a beaker with 20 mL of distilled water, and measuring the time it took to become fully wet [18]. The swelling capacity (CS) was obtained from the ratio between volume occupied by 1 g of sample and that after hydration for 18 h at 25 °C [19,20]. Water holding capacity (WHC) is defined as the amount of water retained by the sample without applying any external force. It was determined by measuring the water content of the precipitate after mixing 0.2 g of sample and 10 mL of distilled water and left to stand for 18 h at 25 °C [19]. Water retention capacity (WRC) is defined as the ability of a sample to retain water after being subjected to an external force such as the centrifuge [19]. For its determination, 1 g of sample was weighed in a graduated conical tube and 10 mL of distilled water was added and left to stand for 18 h at 25 °C. After this time, it was centrifuged for 30 min at 2000 rpm, the supernatant was removed, and the sedimented residue was weighed. The oil retention capacity was evaluated following the methodology proposed by Garau et al. [21]. First, 0.2 g of sample and 1.5 g of sunflower oil were mixed and left to stand overnight at 20 °C. After that, the mix was centrifuged at 3416 rpm for 5 min, and with a Pasteur pipette the supernatant was removed and the weight of the residue was obtained. The oil retention capacity was evaluated based on the increase in the weight of the sample, and the results were expressed in g of oil absorbed by g of the initial sample. The emulsifying activity was determined following the methodology proposed by Yasumatsu et al. [22]. To carry out the procedure, a 2% (*w/v*) sample-water solution was prepared. Next, 7 mL of this

solution was mixed with 7 mL of sunflower oil and homogenized for 5 min in a vortex at 2400 rpm. Finally, it was centrifuged at 10,000 rpm for 5 min and the volume of the emulsion formed was calculated by the ratio between the emulsion volume and the total fluid volume. Emulsifying stability was determined following the methodology proposed by Yasumatsu et al. [22]. For this, a 2% (*w/v*) sample-water solution was prepared. Then, 7 mL of this solution was mixed with 7 mL of sunflower oil and homogenized for 5 min in a vortex at 2400 rpm. Finally, it was heated to 80 °C for 30 min, allowed to cool, and centrifuged at 2000 rpm for 5 min. Emulsifying stability was calculated as the ratio between the emulsion volume and the total fluid volume.

2.3. Particle Size

The particle size of almond bagasse powders was determined by the wet method. Laser diffraction equipment (Masterizer, Malvern Instruments Limited, Worcester, UK) with a measurement range between 0.02 and 200 microns equipped with a blue light of 470 nm wavelength was used. A small amount of sample was diluted in deionized water until reaching an obscuration of 8–9%. Finally, the particle size distribution was obtained and was characterized by the mean diameter of equivalent volume (D [3,4]), equivalent diameter calculated from the area of the particles (D [2,3]), and, finally, d90, d50 and d10, representing the percentiles of the distribution, i.e., the volume of particles below 90%, 50%, and 10% of the particles analyzed, respectively.

2.4. Optical Properties

The CIE*L*a*b* coordinates were measured with a spectrocolourimeter (MINOLTA, CM-3600D, Japan), considering the standard light source D65, the 10° standard observer, and the surface reflectance spectra between 400 and 700 nm. The chroma (C_{ab}) and the color differences (ΔE) of the powders compared to almond bagasse were calculated using Equations (4) and (5), respectively.

$$C_{ab} = \sqrt{a^2 + b^2} \tag{4}$$

$$\Delta E = \sqrt{(\Delta L^*)^2 + (\Delta a^*)^2 + (\Delta b^*)^2} \tag{5}$$

2.5. Antiradical Capacity and Total Phenols Content

For the extraction of phenols and other components with antiradical capacity, a methanol-water mixture 80:20 (*v*/*v*) was prepared and used as a solvent in the relation 1 g sample/100 mL solvent. After 1 h of magnetic stirring, the mix was centrifuged (Selecta, "Medrifriger BL-S") at 10,000 rpm for 5 min at 20 °C. Determinations were made on the supernatant, hereinafter referred to as extract.

2.5.1. Total Phenol Content

The determination of total phenols was performed following the colorimetric method of Folin–Ciocalteu [23]. In a spectrophotometry bucket, 0.125 mL of extract, 0.125 mL of the Folin–Ciocalteu reagent (Sigma-Aldrich, Darmstadt, Germany) and 0.5 mL of bidistilled water were added in that order and allowed to react for 6 min. After this time, 1.25 mL of 7% (*m*/*v*) sodium carbonate solution and 1 mL of distilled water were added. As a reference, a target was used where the sample was replaced by bidistilled water and allowed to react for 90 min. Finally, the absorbance was measured at 765 nm in a spectrophotometer (Thermo Scientific, Helios Zeta U/Vis). The results obtained were compared to a standard curve of gallic acid (purity ≥ 98%, Sigma-Aldrich) and expressed as mg of gallic acid equivalents/g of dry matter (mg GAE/g dm).

2.5.2. Antiradical Capacity by DPPH and ABTS Methods

The antioxidant capacity was determined following the DPPH method described by Stratil et al. [24] with some modifications. First, 0.1 mL of the extract and 2.9 mL of the methanol-DPPH solution (0.394 of DPPH reagent/mL methanol) were mixed and absorbance was measured at 517 nm in a spectrophotometer (Thermo Scientific, Helios Zeta U/Vis). The results were expressed as mg of trolox equivalent/g of dry matter (mg TE/g dm) using the Trolox calibration line ($C_{14}H_{18}O_4$, purity $\geq$ 7%, Sigma-Aldrich) as the reference standard antioxidant, for the range of concentrations between 0 and 500 mg/L.

The antioxidant activity was also evaluated by the ABTS radical method (2,20-azobis-3-ethyl benzothiazolin-6-sulfonic acid) [25]. A solution including the radical ABTS 7 mM and potassium persulfate 2.45 mM in distilled water was prepared and incubated in darkness at room temperature for 16 h. Once this time had elapsed, a dilution with phosphate buffer was carried out to reach an absorbance of 0.7 $\pm$ 0.02 at 734 nm. Then, in a spectrophotometry bucket, 0.1 mL of extract with 2.9 mL of ABTS solution was reacted. As a reference, a white where the sample was replaced by bidistilled water was prepared. The absorbance was measured after 0, 3 and 7 min of reaction at a wavelength of 734 nm in a spectrophotometer (Thermo Scientific, Helios Zeta UV/Vis). The results were expressed as mg of trolox equivalent/g of dry matter (mg TE/g dm), using the Trolox calibration line ($C_{14}H_{18}O_4$, purity $\geq$ 7%, Sigma-Aldrich) as the reference standard antioxidant for the range of concentrations between 0 and 500 mg/L.

2.6. Sorption Isotherms

Sorption isotherms were determined following the gravimetric method described by Wolf et al. [26]. This method uses saturated salt solutions to keep a known and controlled humidity environment within a closed vessel at specific temperature conditions. First, 1 g of sample was placed in a closed jar at 20 °C together with one of the next saturated salt solutions: LiCl (a_w = 0.1), CH_3COOK (a_w = 0.23), $MgCl_2$ (a_w = 0.32), K_2CO_3 (a_w = 0.43), $Mg(NO_3)_2$ (a_w = 0.52), NaCl (a_w = 0.75), KCl (a_w = 0.85), and $BaCl_2$ (a_w = 0.90). The samples were weighed every eight days until a constant weight was reached.

2.7. Statistical Analysis

The results were statistically analyzed with Statgraphics software (Centurion XVI.I, Statpoint Technologies, Inc., Warrenton, VA, USA) at a 95 % confidence level (p-value $\leq$ 0.05). The normality of the data was tested with the Shapiro–Wilk test (p > 0.05). The data were processed by simple ANOVA after checking the normality of the data. For each processing treatment, three different experiments with three replicates each were carried out. Significant differences (p-value < 0.05) among groups were determined by Fisher's LSD test.

3. Results and Discussion

3.1. Properties of Almond Bagasse Powders

Table 1 shows the composition, physico-chemical, water interaction, emulsifying properties, and color of fresh, air dried, and freeze-dried almond bagasse powders. Dehydration, in all cases, reached a water activity lower than 0.3, which is the recommended limit to ensure the stability of powdered products [27,28]. Although the water activity limit for microbial growth is 0.90 for most bacteria and 0.87 and 0.75 for most yeasts and fungi, a water activity limit lower than 0.3 assures kinetic stability in powdered products since it is guaranteed that there is no free water that can participate in chemical and enzymatic reactions. The moisture content in the final samples was low, as isotherms showed a very low water binding capacity (see isotherms section). Thus, more than 98% of the water is easily removed during drying.

Considering the fat and protein content, the almond bagasse retained a high percentage of fat and protein from fresh almond and there were no significant differences between fresh and dehydrated samples. Fat content remained around 25% (0.25 g/g_{dm}) in the bagasse and protein reached 16–17% (0.16–0.17 g/g_{dm}); the initial values in fresh almond

were around 54% and 25%, respectively [29]. In a study carried out with fresh baru almond, fat content around 39–43% was reported, and the protein content was around 23–28%, slightly higher than those obtained for almond bagasse [30]. Compared with other cereal by-products of interest to the food industry, protein content was similar to those obtained in rice bran (0.14 g protein/g) [31], oat bran (0.17 g protein/g) [32], by-product from tofu (0.15 g protein/g) [33], and soybean residue (0.15 g protein/g) [33], but lower than that for fresh okara (0.39 g protein/g) [34] and rice bran (0.22 g protein/g) [35]. Particular attention should be paid to the fat content. Stability in low-moisture, fat-containing foods is highly dependent on the characteristics of the matrix, its microstructure, and the presence of other macronutrients such as protein. Oxidation mechanisms are complex and need to be studied on a case-by-case basis to ensure proper packaging and storage [36].

Table 1. Composition, physico-chemical, water interaction, emulsifying properties and color of fresh almond bagasse and, air dried (HAD60: hot air dried at 60 °C; HAD70: hot air dried at 70 °C) and freeze-dried (LYO) almond bagasse powders. The values in brackets for fresh bagasse refer to the composition expressed in g/g of raw material. Mean ± standard deviation of three repetitions. Different superscripts letters in the same line indicate statistically significant differences with a confidence level of 95%. $_{dm}$, dry matter; $_{w}$, water; X_w, water content; X_{ss}, soluble solids content; WHC, water holding capacity; WRC, water retention capacity.

	FRESH	HAD60	HAD70	LYO	*p*-Value
Physico-chemical properties					
a_w	0.99 ± 0.08 ^{a}	0.23 ± 0.04 ^{b}	0.20 ± 0.06 ^{bc}	0.13 ± 0.02 ^{c}	0.0000
Fat (g/g_{dm})	0.25 ± 0.002 ^{a} (0.11)	0.252 ± 0.002 ^{a}	0.253 ± 0.004 ^{a}	0.250 ± 0.006 ^{a}	0.7106
Protein (g/g_{dm})	0.15 ± 0.03 ^{a} (0.07)	0.16 ± 0.04 ^{b}	0.16 ± 0.03 ^{b}	0.165 ± 0.008 ^{b}	0.0030
X_w (g/g_{dm})	1.262 ± 0.011 ^{b} (0.558)	0.014 ± 0.002 ^{a}	0.015 ± 0.012 ^{a}	0.02 ± 0.08 ^{a}	0.0000
Ashes (g/g_{dm})	0.031 ± 0.011 ^{a} (0.014)	0.031 ± 0.007 ^{a}	0.03 ± 0.06 ^{a}	0.030 ± 0.012 ^{a}	0.0000
Fiber Van Soest (g/g_{dm})	0.47 ± 0.02 ^{a} (0.21)	0.45 ± 0.02 ^{a}	0.50 ± 0.03 ^{a}	0.50 ± 0.03 ^{a}	0.6605
Cellulose and lignine (g/g_{dm})	0.17 ± 0.02 ^{a} (0.08)	0.20 ± 0.05 ^{ab}	0.20 ± 0.15 ^{ab}	0.21 ± 0.02 ^{b}	0.0005
Hemicellulose (g/g_{dm})	0.23 ± 0.04 ^{a} (0.10)	0.260 ± 0.014 ^{a}	0.290 ± 0.012 ^{a}	0.295 ± 0.002 ^{a}	0.0008
X_{ss} (g_{ss}/g_{dm})	0.013 ± 0.003 ^{a} (0.006)	0.013 ± 0.004 ^{a}	0.013 ± 0.004 ^{a}	0.014 ± 0.004 ^{a}	0.6810
Water interaction properties					
Solubility (%)	-	29 ± 1 ^{b}	26.2 ± 2.2 ^{a}	30.1 ± 1.1 ^{c}	0.0000
Hygroscopicity (g_w/g)	-	0.17 ± 0.06 ^{a}	0.17 ± 0.17 ^{a}	0.17 ± 0.03 ^{a}	0.9763
Wettability (s)	-	8.3 ± 1.1 ^{a}	8.9 ± 0.6 ^{a}	8.3 ± 1.1 ^{a}	0.7458
Swelling capacity (mL_w/g)	-	4.51 ± 0.08 ^{a}	4.51 ± 0.08 ^{a}	4.51 ± 0.08 ^{a}	1.0000
WHC (g_w/g_{dm})	-	2.9 ± 0.5 ^{a}	2.6 ± 0.2 ^{a}	8.4 ± 1.8 ^{b}	0.0009
WRC (g_w/g_{dm})	-	4.5 ± 0.2 ^{a}	4.6 ± 0.2 ^{a}	5.91 ± 0.08 ^{b}	0.0000
Oil interaction properties					
Oil retention ability (g_o/g_s)	-	2.3 ± 0.5 ^{a}	2.6 ± 0.2 ^{a}	4.2 ± 0.06 ^{b}	0.0047
Emulsifying activity (%)	-	19 ± 2 ^{a}	20 ± 2 ^{a}	34 ± 2 ^{b}	0.0002
Emulsifying stability (%)	-	20 ± 2 ^{a}	24 ± 2 ^{a}	59 ± 2 ^{b}	0.0000
Colour					
L	73.68 ± 0.07 ^{a}	62.358 ± 0.010 ^{c}	58.236 ± 0.002 ^{d}	66.561 ± 0.001 ^{b}	0.0010
a*	4.88 ± 0.02 ^{d}	4.999 ± 0.009 ^{c}	6.487 ± 0.009 ^{a}	6.039 ± 0.002 ^{b}	0.0039
b*	11.62 ± 0.04 ^{d}	14.279 ± 0.006 ^{c}	16.143 ± 0.017 ^{a}	15.026 ± 0.014 ^{b}	0.0030
C	12.61 ± 0.05 ^{d}	15.128 ± 0.08 ^{c}	17.398 ± 0.014 ^{a}	16.194 ± 0.012 ^{b}	0.0204
ΔE	-	11.625 ± 0.010 ^{b}	16.167 ± 0.003 ^{a}	7.971 ± 0.06 ^{c}	0.0001

According to the fiber content, no significant differences among treatments or fresh almond bagasse were detected. Van Soest fiber includes cellulose and lignin as insoluble fraction and the hemicellulose as a more soluble one. Values of total fiber were above those reported for okara fresh matter (13.84 g/100 g) [37], rice bran (28.6 g/100 g) [35], and oat bran (15.55 g/100 g of dry matter) [32], but they were below those of other by-products,

such as by-product from tofu (58.6 g/100 g of dry matter) [33], bran fiber rice (53.25 g/100 g of dry matter) [35], or solid by-product tiger nut (59.71 g/100 g) [38], and similar to carrot skin (45.45–49.23 g/100 g of dry weight) [39]. Soluble dietary fibers such as pectin cannot be quantified by the fiber determination method used. However, this fraction could be estimated by the difference between the total mass and the total of the macronutrients considered. As the sum of fat, protein, fiber and water is 100%, the more soluble fiber including pectin can be considered negligible. Almond bagasse powders could be used as ingredients promoting intestinal transit more than an ingredient conferring viscosity since high content in soluble than insoluble was fiber observed in all cases. Soluble fiber is the one that confers viscosity properties, ability to form gels, and emulsifying capacity, while insoluble fiber with a greater porosity and lower density promotes intestinal transit [40].

Water solubility values ranged from 26.2% to 30.1%, without significant differences between hot air-dried and freeze-dried samples. The freeze-dried samples showed slightly high solubility levels, presumably caused by the more severe structural damage induced by the freezing and subsequent water sublimation during lyophilization. An increase in the air-drying temperature resulted in a decrease in solubility, probably due to physical changes affecting macromolecules during the drying process. These physical changes during hot air drying could promote the formation of a surface crust, which can hinder the interaction between molecules and water [41]. Solubility values were lower when compared to those from other fruit powders such as passion fruit (44.6% to 57.56%) [42] or pineapple juice powder (81.56%) [43]. Nevertheless, the results were closer to those obtained for oat bran (ranging from 11.70% to 26.32% depending on the drying process applied) [44]. Clearly, a higher percentage of macromolecules such as insoluble fiber and proteins in the composition of by-products such as bran or bagasse provides lower solubilities. Additionally, the presence of a high percentage of fat makes the interaction with water molecules even more difficult.

Hygroscopicity is the capacity of a material or powder to absorb moisture and come into equilibrium with the relative humidity of the environment. The low water content of food powders could contribute to their high hygroscopicity, which gives rise to sticky and caked powders with low porosity, therefore decreasing their ability to rehydrate and retain aromas [45]. Food powder is considered good if it has low hygroscopicity [45]. According to Callahan et al. [46], a material can be considered non-hygroscopic when an increase of less than 20% (w/w) in moisture content above 90% relative humidity is observed after one week. Almond bagasse powder gained 0.17 g of water/g (17%) when equilibrated at 97% relative humidity after one week and was therefore non-hygroscopic. Non-significant differences were observed among the samples.

Wettability, swelling capacity, the water holding capacity (WHC), and the water retention capacity (WRC) are largely conditioned by the particle size and composition, mainly the fiber type and fat content. Wettability and the swelling capacity of almond bagasse powders were not significantly affected by the drying method or air temperature. However, WHC and WRC are significantly higher in the lyophilized powders. A different size distribution (Figure 1) with a single peak indicative of a larger volume of larger particles could be the explanation for these differences. According to Bai et al. [44], the larger the particle size, the higher the wettability since water molecules can permeate through the larger voids left between the particles. Regarding composition, soluble fiber has a high capacity to retain water and expand to form a viscous solution, while insoluble fiber can also absorb and retain water in its fibrous matrix but in a lower quantity; fat, on the other hand, hinders any interaction with water. Lecumberry et al. [47] reported results for WRC in apple and orange pectin of 16.51 $\pm$ 3.77 and 28.07 $\pm$ 5.37 g water/g dry matter, respectively), these results being higher than those obtained for almond bagasse, which is consistent with the higher content of insoluble fiber and the presence of fat in the almond bagasse. Nevertheless, similar results were obtained in lulo bagasse (8.2 $\pm$ 0.7), a material also with a high content of insoluble fiber [48]. Bai et al. [44] provided data on WHC in

oat bran (5.95 to 6.48 g of water/ g of dry matter), which were similar to those obtained in freeze-dried almond bagasse and slightly lower in hot air-dried powders.

	D [4,3]	D [3,2]	d (0.1)	d (0.5)	d (0.9)
HAD60	112 ± 3^{a}	25.8 ± 0.3^{a}	12.3 ± 0.1^{a}	81 ± 1^{a}	264 ± 9^{a}
HAD70	120 ± 4^{ab}	26.4 ± 0.3^{a}	12.6 ± 0.1^{a}	81 ± 2^{a}	291 ± 12^{b}
LYO	125 ± 11^{b}	26.0 ± 0.8^{a}	11.9 ± 0.4^{b}	94 ± 3^{b}	282 ± 25^{ab}
p-value	0.0334	0.1524	0.0032	0.0000	0.0451

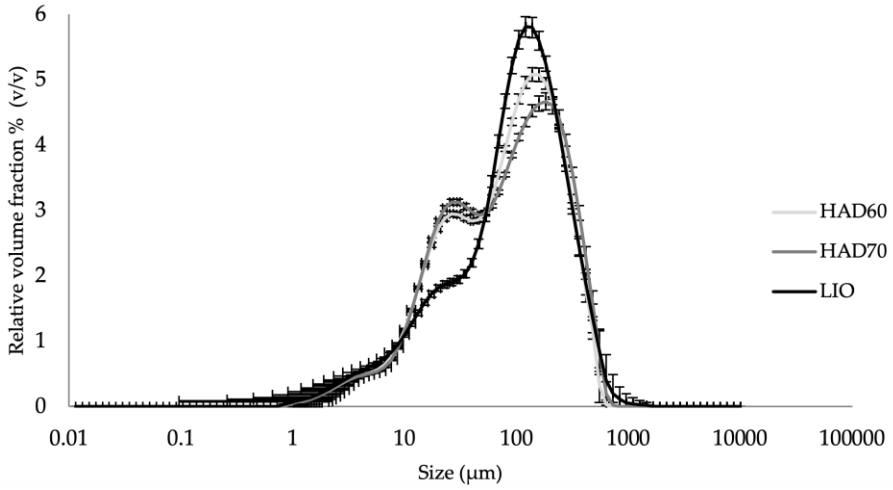

Figure 1. Particle size of hot air dried (HAD60: hot air dried at 60 °C; HAD70: hot air dried at 70 °C) and freeze-dried (LYO) almond bagasse powders. Mean ± standard deviation of five repetitions. Different superscripts letters in the same column indicate statistically significant differences with a confidence level of 95%.

Regarding oil interaction properties, the results obtained for almond bagasse powders showed good emulsifying properties, such as emulsifying activity and emulsifying stability. Significant differences were detected between freeze-dried and air-dried samples, regardless of air temperature. The values obtained for freeze-dried powders were higher (Table 1). The emulsifying capacity is associated with the presence of hydrophilic and hydrophobic groups. The high protein content present in the almond bagasse justifies its good oil-interaction properties. In freeze-dried samples, the increased structural damage caused by freezing and sublimation contributes to the breakdown of complex molecules, leaving more hydrophilic and hydrophobic groups available for interaction and consequently improving the oil-interaction properties [49]. Regarding oil retention ability, similar values were reported for commercial fibers from lemon, orange, peach, apple, and persimmon (2.5 to 2.9 g oil/ g sample) [50]. Similar emulsion stability to that of freeze-dried almond bagasse powder was obtained for peas (59.4% ± 1.0) and lentils (55.0% ± 2.5). The emulsifying activity of almond bagasse could be compared with the results obtained for peas (40.9% ± 0.7) and lentils (39.9% ± 1.0) [51].

Associated with browning and oxidation reactions, all samples experienced color differences when compared to the fresh almond bagasse (Table 1). These changes gave the samples more yellowish-red tones, denoted by higher values of the a^* and b^* coordinates. The saturation (C) in all cases shows a low value, being lower in the fresh bagasse. According to Bodart et al. [52], color differences are imperceptible to the human eye when they are $\Delta E < 1$. Small differences can be seen when $1 < \Delta E < 3$ and will be visibly evident when the value of $\Delta E > 3$. Since in all samples the values were higher than 3, the changes were clearly perceptible. However, the color difference in the freeze-dried powder was smaller since freeze-drying occurs under vacuum and at low temperatures, minimizing oxidation processes.

Figure 1 shows the particle size distribution and characteristic parameters of hot air-dried and freeze-dried almond bagasse powders. Practically, a monomodal distribution for the freeze-dried powder and a bimodal distribution for air-dried powders were observed. In the freeze dried, the structural breakdown induced by/100 g water freezing and sublimation resulted in a more homogeneous particle size distribution and a slight shift in the maximum towards a smaller particle size. Probably, in hot air-dried samples, phase transitions in macromolecules such as carbohydrates and proteins, and their different mechanical resistance to crushing, resulted in a more heterogeneous distribution, and specifically a bimodal one. This distribution is quite common in carbohydrate and fiber-rich powders produced by hot-air drying, such as blueberry powder and the tangerine skin powder dried at 70 °C [53,54].

Regarding antioxidant properties (Table 2), the highest values of antiradical activities were obtained for fresh samples. No significant differences were observed between the different drying methods and temperatures used. The total phenols of the freeze-dried samples were very similar to those of the fresh samples. Freeze-drying occurs at low temperature and in vacuum conditions, which contributes to maintaining bioactive compounds with anti-radical activity such as phenols [40]. In hot air-drying treatments, structural damage and the presence of oxygen at high temperature resulted in higher degradation. However, for the inactivation of enzymes involved in some of the degradation reactions, the difference between 60 and 70 °C could be decisive. In terms of interaction with other molecules, it has been shown that dehydration can increase polyphenolic compounds, despite some degradation, because it can improve extraction and lead to a greater release of these compounds [55]. In almond bagasse, the macronutrient composition, consisting mainly of fiber and fat, could interact with the polyphenols and prevent them from getting released after processing. Comparing results from the DPPH and ABTS methods, the ABTS radical reacted with more antioxidant compounds. The lower reaction time of ABTS radical and its more hydrophilic nature enabled it to react in both organic and aqueous media.

Table 2. Total phenols content and antiradical capacity by DPPH and ABTS methods of fresh almond bagasse and, hot air-dried (HAD60: hot air-dried at 60 °C; HAD70: hot air-dried at 70 °C) and freeze-dried (LYO) almond bagasse powders. Mean ± standard deviation of three repetitions. Different superscripts letters for the same determination indicate statistically significant differences with a confidence level of 95%. $_{dm}$, dry matter; GAE, acid gallic equivalents; TE, Trolox equivalent.

	FRESH	HAD60	HAD70	LYO	*p*-Value
Total phenols (mg GAE/g_{dm})	0.59 ± 0.03 ^{a}	0.291 ± 0.012 ^{b}	0.33 ± 0.02 ^{b}	0.5 ± 0.2 ^{ab}	0.0000
DPPH (mg TE/g_{dm})	0.67 ± 0.06 ^{a}	0.296 ± 0.007 ^{b}	0.31 ± 0.03 ^{b}	0.32 ± 0.05 ^{b}	0.0154
ABTS (mg TE/g_{dm})	2.9 ± 0.2 ^{a}	0.96 ± 0.03 ^{b}	1.03 ± 0.07 ^{b}	1.121 ± 0.012 ^{b}	0.0000

The values for total phenols were quite similar to those reported for almond shell, ranging from 0.86 to 1.16 mg GAE/gdm [56], but higher values were found in fresh almonds (2.87 mg GAE/gdm), brazil nuts (2.44 mg GAE/gdm), hazelnuts (6.87 mg GAE/gdm), and pecans (1,81 mg GAE/gdm) [57]. Similar results were obtained in peach (0.51 mg GAE/gdm), fig (0.59 mg GAE/gdm), macadamias (0.46 mg GAE/gdm), and pines (0.32 mg GAE/gdm) [58,59].

3.2. Air Drying Kinetics

Figure 2 shows the drying and drying rate curves of thin-layer air-drying of almond bagasse at 60 and 70 °C. The almond bagasse was dried from the initial moisture of 55% to a final value of around 5.5%. The time needed to reduce the water content was 4.5 and 3.7 h at 60 and 70 °C, respectively. As expected, the statistical analysis revealed the significant effect (p-value < 0.05) of air temperature on water content removal during the process.

When the air temperature increased, it had a greater capacity to retain water, promoting the drying process. At the same time, the temperature of the bagasse increased significantly, increasing the water diffusivity from the inner layers to the surface [60]. Furthermore, Ling et al. [61] suggested that in pasty products, such as sludge, this temperature increase was linked to a porosity reduction. Fresh almond bagasse was slightly pasty, so the reduction in porosity could have also contributed to the increase in the drying rate.

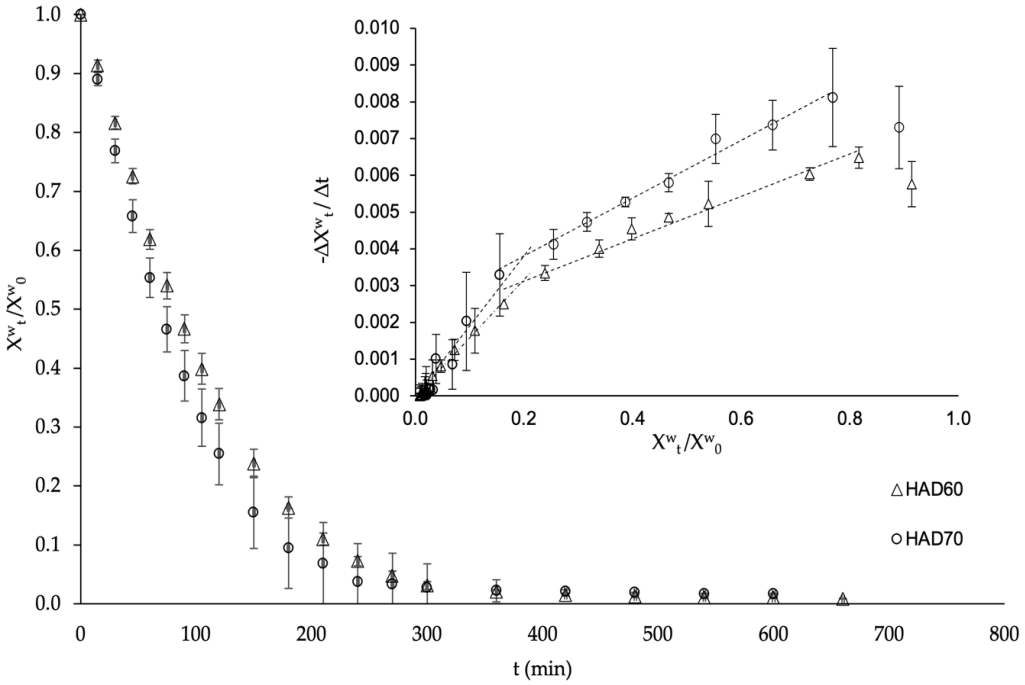

Figure 2. Air drying curves of almond bagasse at 60 and 70 °C. In the nested figure, the drying rate curves and the linear fits of the experimental data at 60 and 70 °C have been plotted. HAD: Hot air drying; X^w: water content (g water/g dry matter); 0, t are referring to initial and any other time. Mean values and standard deviation of three repetitions have been represented.

During the first few minutes of the air-drying process, the drying rate increased until it reached the highest value (Figure 2). This increase was associated with the progressive heating of the product when it comes into contact with the hot air. The experimental data revealed that this stage, which corresponds to the induction stage, had a duration of 20–30 min, depending on the drying temperature. After the induction period, in high moisture foods, a water-free layer over the entire surface of the food usually results in a constant drying rate [62]. However, the initial moisture content of the fresh bagasse was around 55%, which was low enough that there was no longer a free layer of water. Thus, drying rate curves revealed that the process at the temperature values took place in the falling rate period entirely. Two periods of declining drying rate were observed; in both cases, the decrease in drying rate was linear with the reduction in moisture ratio $\frac{Xw}{Xw_0}$. Therefore, it could be said that the drying process was controlled by internal water diffusion. In the first stage, when the bagasse had the higher water content, the reduction in velocity was lower than in the second stage when the bagasse was almost dry. This behavior was largely influenced by the composition and structural characteristics of the bagasse. Considering that the main components of the bagasse do not have a high water-holding capacity (this will be discussed later in the sorption isotherms section), it can be stated that its structural characteristics, in particular its porosity and particle size, determined the facility with which water molecules were removed. Additionally, the extent of compartmentalization associated with the crushing level influences physical interactions that also affect the rate of the process.

Modelling the drying curves and obtaining the kinetic parameters provides information on the mechanisms involved. Furthermore, it makes it possible to control the process by improving energy consumption and subsequently optimize the drying process for greater efficiency and a better quality final product. Numerous models have been used by researchers [63]. These are theoretical, semi-theoretical, and empirical models that usually correlate the moisture ratio with the drying time. Theoretical models provide insights to the mechanisms involved in water loss but offer complex mathematical solutions that are difficult to fit and manage. On the other hand, empirical models provide simple and fast solutions that are effective for practical operation management when the experimental conditions under which they are obtained correspond to the real operating conditions. Semi-theoretical models are the most applied and are generally derived from a direct solution of Fick's second law by assuming some simplifications.

In this study, the experimental data were fitted to an empirical model that establishes a linear correlation between the drying rate and the moisture ratio and to the simplified diffusional model, considering a single term of the serial progression from the integration of Fick's second law (Table 3). The simplified diffusional model usually fits well when drying occurs in the falling rate, as this is when the predominant mechanism is the diffusion of water from the innermost layers of the food samples to the surface. In the application of the equation, it was assumed that water diffusion occurred in a single direction and remained constant, the material was isotropic, and the moisture distribution uniform. The external resistance to water transport was negligible compared to the internal resistance and there was no shrinkage or swelling of the food material. The adjustment allowed the calculation of the effective moisture diffusivity (De) as a kinetic parameter to compare the facility with which water diffuses from the inner part of the bagasse to the outer part. The values obtained were 1.97×10^{-9} and 2.18×10^{-9} m^2/s for the temperatures of 60 and 70 °C, respectively. These values are within the range generally given for the moisture diffusion of food materials (10^{-11} to 10^{-6} m^2/s) [64,65].

Table 3. Air drying kinetics of almond bagasse at 60 and 70 °C. $\frac{X^w - X^w_\infty}{X^w_c - X^w_\infty}$: Dimensionless moisture ratio, $\frac{Xw}{Xw_0}$: Moisture ratio, $\frac{\Delta Xw}{\Delta t}$: Drying rate, De: Effective water diffusivity, L: Half-thickness of bagasse thin layer, t: time, R^2: Correlation coefficient, RMSE: Root mean square error, MRE: Mean relative error.

	Model equation	**60 °C**	**70 °C**
Linear empirical model	Stage 1 $\frac{\Delta Xw}{\Delta t} = k_1 \frac{Xw}{Xw_0} + k_2$	$\frac{Xw}{Xw_0} \in \lfloor 0.816,\ 0.2 \rfloor$	$\frac{Xw}{Xw_0} \in \lfloor 0.769,\ 0.18 \rfloor$
	k_1	0.006	0.008
	k_2	0.002	0.002
	R^2	0.971	0.983
	RMSE	6.40×10^{-4}	9.36×10^{-5}
	MRE	0.049	0.031
	Stage 2 $\frac{\Delta Xw}{\Delta t} = k'_1 \frac{Xw}{Xw_0}$	$\frac{Xw}{Xw_0} \in \lfloor 0.2,\ 0.02 \rfloor$	$\frac{Xw}{Xw_0} \in \lfloor 0.18,\ 0.022 \rfloor$
	k'_1	0.016	0.019
	R^2	0.995	0.921
	RMSE	1.26×10^{-5}	1.05×10^{-4}
	MRE	0.194	0.207
Difusional model	$\frac{X^w - X^w_\infty}{X^w_c - X^w_\infty} = \frac{8}{\pi^2} e^{\left(-\frac{D \cdot \pi^2 \cdot t}{4 \cdot L^2}\right)}$	$\frac{Xw}{Xw_0} \in \lfloor 0.816,\ 0.02 \rfloor$	$\frac{Xw}{Xw_0} \in \lfloor 0.769,\ 0.022 \rfloor$
	De (m^2/h)	7.11×10^{-6}	7.88×10^{-6}
	R^2	0.993	0.983
	RMSE	0.039	0.033
	MRE	0.331	0.310

Saravacos and Maroulis [66] investigated the effect of food properties on the drying kinetics of non-cellular structured food. They established the important effect of food structure and hygroscopicity and reported typical values of effective water diffusivity, varying from 50 to 0.01 $\times$ 10^{-10} m^2/s depending on hygroscopicity. Xiong et al. [67] showed that the effective diffusivity (De) was higher in pregelatinized samples and was found to be much higher through porous puffed pasta than regular pasta. Ruimin et al. [68] found that the total drying time of sludge particles with a diameter of 10 mm is not much different from that of particles with a diameter of 6 mm, while the total drying time of particles with a diameter of 18 mm increases significantly.

The goodness of the fit was determined by the correlation coefficient (R^2), the root mean square error (RMSE), and the mean relative error (MRE). It is generally accepted that an R^2 value higher than 0.93 and an MRE lower than 0.1 are good fits. Although, the MRE of the fit to the simplified diffusional Fick's model is too high, the correlation coefficient is good and could be accepted as an acceptable approach. In the case of the linear empirical model, the fit was more accurate.

3.3. Sorption Isotherms

Figure 3 shows the moisture sorption isotherms at 20 °C of hot air-dried almond bagasse powder at 60 °C (HAD60), at 70 °C (HAD70), and the freeze-dried one (LYO).

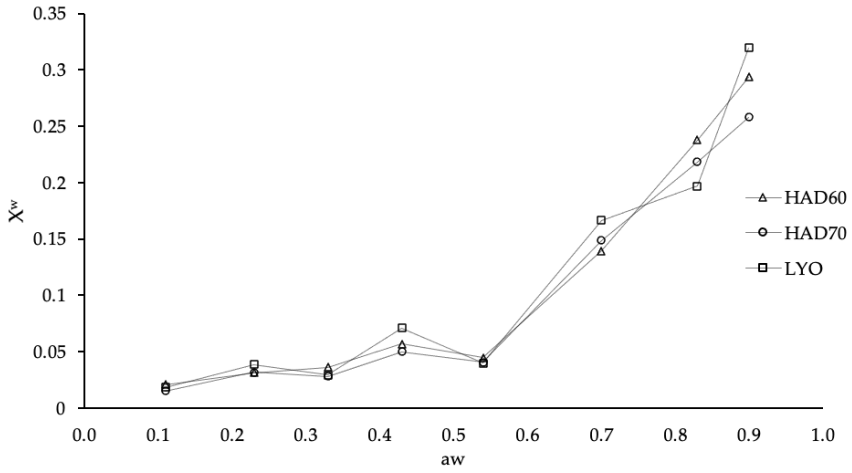

Figure 3. Sorption isotherms of hot air-dried (HAD60: hot air-dried at 60 °C; HAD70: hot air-dried at 70 °C) and freeze-dried (LYO) almond bagasse powders at 20 °C. X^w: water content (g water/gdm).

It can be observed that at rather low moisture values (~0.3 g water/g dry matter), water activity values of 0.9 are reached. The isotherm is very close to the x-axis, which indicates that the product has a very low water binding capacity, possibly influenced to a large extent by its fat content. Two practically linear sections can be identified; a rather flat first section for water activities equal to or less than 0.54, and a second section with a positive slope for water activities equal to or greater than 0.54 This results in a type III isotherm, which is quite common in non-porous foods. This shape appears when the net heat of sorption is small (specifically with a BET C value of less than 2). A small net heat of sorption indicates that the interactions between the water and the other components are weak and more linked to physical than chemical phenomena [69].

When comparing the isotherm with that obtained for raw almond powder [70], the typical plateau at very low a_w has disappeared. This plateau is associated with high water adsorption by complex molecules with many active points, such as carbohydrates or soluble proteins. These have been extracted during the production process of vegetable almond drink and are no longer present in the bagasse.

In powdered products, physical and chemical sorption phenomena are largely conditioned by the macromolecular structure of the product as well as by its chemical composi-

tion and the physical state of its components [71]. Regarding the macromolecular structure, in all cases, a powder with large and slightly caked particles was obtained, which greatly limits the adsorption phenomena. Considering the composition, the fat content, which is hydrophobic in nature, together with insoluble long-chain carbohydrates (insoluble fibre constituted mainly of cellulose and lignin) is high, and the water adsorption capacity is low. Furthermore, the drying processes applied, such as hot air drying and freeze-drying, may have induced phase transitions aimed at the crystallization of some molecules, resulting in very small or zero stoichiometric hydration contents.

4. Conclusions

Hot air drying and freeze-drying were found to be suitable processes for obtaining a plant-based powder from the bagasse resulting from the production of vegetable almond drink. In all cases, a nutritious powder was obtained with low water binding capacity and therefore good properties for packaging and storage. However, due to its high fat content, it is worth studying its stability when stored. No clear trend was observed for the effect of the drying method (hot air or freeze-drying) on total phenolic content, antiradical capacity, physico-chemical properties, or interaction with water or oil. However, faster kinetics at 70 °C resulted in higher industrial productivity. Freeze-drying resulted in a powder with a more homogeneous particle size distribution and better oil-interaction properties, especially with higher emulsifying activity and stability. It would be the most recommended process to obtain a powder with emulsifying properties.

Author Contributions: Conceptualization, N.B.; methodology, N.B., S.D. and E.B.; data curation, S.D.; writing—original draft preparation, N.B. and S.D.; writing—review and editing, N.B., E.B., C.B. and L.S.; funding acquisition, N.B. All authors have read and agreed to the published version of the manuscript.

Funding: This research was funded by Universitat Politècnica de València, Ayuda PAID-11-21.

Conflicts of Interest: The authors declare no conflict of interest. The funders had no role in the design of the study; in the collection, analyses, or interpretation of data; in the writing of the manuscript; or in the decision to publish the results.

References

1. MAPA Ministerio de Agricultura, Pesca y Alimentación. Available online: https://www.mapa.gob.es/en/alimentacion/temas/desperdicio/ (accessed on 20 January 2023).
2. Feng, J.Y.; Wang, R.; Thakur, K.; Ni, Z.J.; Zhu, Y.Y.; Hu, F.; Zhang, J.G.; Wei, Z.J. Evolution of Okara from Waste to Value Added Food Ingredient: An Account of Its Bio-Valorization for Improved Nutritional and Functional Effects. *Trends Food Sci. Technol.* **2021**, *116*, 669–680. [CrossRef]
3. Trabold, T.A.; Rodríguez Alberto, D. Valorization of Food Processing By-Products via Biofuel Production. In *Sustainability of the Food System*; Academic Press: Cambridge, MA, USA, 2020; pp. 53–69. [CrossRef]
4. de Souza, T.S.P.; Dias, F.F.G.; Koblitz, M.G.B.; de Moura Bell, J.M.L.N. Effects of Enzymatic Extraction of Oil and Protein from Almond Cake on the Physicochemical and Functional Properties of Protein Extracts. *Food Bioprod. Process.* **2020**, *122*, 280–290. [CrossRef]
5. Saba, B.; Bharathidasan, A.K.; Ezeji, T.C.; Cornish, K. Characterization and Potential Valorization of Industrial Food Processing Wastes. *Sci. Total Environ.* **2023**, *868*, 161550. [CrossRef]
6. Lorente, D.; Duarte Serna, S.; Betoret, E.; Betoret, N. Opportunities for the Valorization of Waste Generated by the Plant-Based Milk Substitutes Industry. In *Advanced Technologies in Wastewater Treatment*; Elsevier: Amsterdam, The Netherlands, 2023; pp. 25–66, ISBN 9780323885102.
7. FAO. El Director General de la Industria Alimentaria Valora la Estabilidad de los Datos de Desperdicio Alimentario en 2019. Available online: https://www.mapa.gob.es/es/prensa/ultimas-noticias/el-director-general-de-la-industria-alimentaria-valora-la-estabilidad-de-los-datos-de-desperdicio-alimentario-en-2019/tcm:30-543935 (accessed on 4 June 2023).
8. Espinosa-Puerta, J.M. Aprovechamiento Integral del Residuo de la Industria de la Almendra. Available online: http://efaidnbmnnnibpcajpcglclefindmkaj/https://crea.ujaen.es/bitstream/10953.1/12079/1/Memoria.JM.Espinosa.pdf (accessed on 20 January 2023).
9. Castellanos Fuentes, A.P.; Bengoa, A.; Gagliarini, N.; Abraham, A.; de Escalada Pla, M.F.; Flores, S.K. Physicochemical and Functional Characterisation of a Food Ingredient Based on Okara Containing Probiotics. *Food Bioprod. Process.* **2022**, *135*, 74–86. [CrossRef]

10. Martins, Z.E.; Pinho, O.; Ferreira, I.M.P.L.V.O. Food Industry By-Products Used as Functional Ingredients of Bakery Products. *Trends Food Sci. Technol.* **2017**, *67*, 106–128. [CrossRef]
11. AOAC 934.06, 1934 AOAC 934.06-1934(1996), Loss on Drying (Moisture) in Dried Fruit: AOAC Official Method. Available online: http://www.aoacofficialmethod.org/index.php?main_page=product_info&products_id=695 (accessed on 11 February 2023).
12. AOAC 991.36, 1996 AOAC 991.36-1996, Fat(Crude) in Meat and Meat Products–Solvent: AOAC Official Method. Available online: http://www.aoacofficialmethod.org/index.php?main_page=product_info&cPath=1&products_id=2528 (accessed on 11 February 2023).
13. AOAC 950.48, 1950 AOAC 950.48-1950, Protein (Crude) in Nuts and Nut Products. AOAC Official Method. Available online: http://www.aoacofficialmethod.org/index.php?main_page=product_info&products_id=836 (accessed on 11 February 2023).
14. Mertens, D.R.; Collaborators. Gravimetric Determination of Amylase-Treated Neutral Detergent Fiber in Feeds with Refluxing in Beakers or Crucibles: Collaborative Study. *J. AOAC Int.* **2002**, *85*, 1217–1240. [CrossRef]
15. AOAC 940.26, 1940 AOAC 940.26-1940, Ash of Fruits and Fruit Products: AOAC Official Method. Available online: http://www.aoacofficialmethod.org/index.php?main_page=product_info&cPath=1&products_id=1447 (accessed on 11 February 2023).
16. Mimouni, A.; Deeth, H.C.; Whittaker, A.K.; Gidley, M.J.; Bhandari, B.R. Rehydration Process of Milk Protein Concentrate Powder Monitored by Static Light Scattering. *Food Hydrocoll.* **2009**, *23*, 1958–1965. [CrossRef]
17. Cai, Y.Z.; Corke, H. Production and Properties of Spray-Dried Amaranthus Betacyanin Pigments. *J. Food Sci.* **2000**, *65*, 1248–1252. [CrossRef]
18. Freudig, B.; Hogekamp, S.; Schubert, H. Dispersion of Powders in Liquids in a Stirred Vessel. *Chem. Eng. Process. Process Intensif.* **1999**, *38*, 525–532. [CrossRef]
19. Raghavendra, S.N.; Rastogi, N.K.; Raghavarao, K.S.M.S.; Tharanathan, R.N. Dietary Fiber from Coconut Residue: Effects of Different Treatments and Particle Size on the Hydration Properties. *Eur. Food Res. Technol.* **2004**, *218*, 563–567. [CrossRef]
20. Robertson, J.A.; De Monredon, F.D.; Dysseler, P.; Guillon, F.; Amadò, R.; Thibault, J.F. Hydration Properties of Dietary Fibre and Resistant Starch: A European Collaborative Study. *LWT-Food Sci. Technol.* **2000**, *33*, 72–79. [CrossRef]
21. Garau, M.C.; Simal, S.; Rosselló, C.; Femenia, A. Effect of Air-Drying Temperature on Physico-Chemical Properties of Dietary Fibre and Antioxidant Capacity of Orange (*Citrus aurantium* v. Canoneta) by-Products. *Food Chem.* **2007**, *104*, 1014–1024. [CrossRef]
22. Yasumatsu, K.; Sawada, K.; Moritaka, S.; Misaki, M.; Toda, J.; Wada, T.; Ishii, K. Whipping and Emulsifying Properties of Soybean Products. *Agric. Biol. Chem.* **2014**, *36*, 719–727. [CrossRef]
23. Wolfe, K.; Wu, X.; Liu, R.H. Antioxidant Activity of Apple Peels. *J. Agric. Food Chem.* **2003**, *51*, 609–614. [CrossRef] [PubMed]
24. Stratil, P.; Klejdus, B.; Kubáň, V. Determination of Total Content of Phenolic Compounds and Their Antioxidant Activity in Vegetables–Evaluation of Spectrophotometric Methods. *J. Agric. Food Chem.* **2006**, *54*, 607–616. [CrossRef]
25. Re, R.; Pellegrini, N.; Proteggente, A.; Pannala, A.; Yang, M.; Rice-Evans, C. Antioxidant Activity Applying an Improved ABTS Radical Cation Decolorization Assay. *Free Radic. Biol. Med.* **1999**, *26*, 1231–1237. [CrossRef] [PubMed]
26. Wolf, W.; Spiess, W.E.L.; Jung, G. Standardization of Isotherm Measurements (Cost-Project 90 and 90 BIS). In *Properties of Water in Foods: In Relation to Quality and Stability*; Springer: Dordrecht, The Netherlands, 1985; pp. 661–679. [CrossRef]
27. Inglett, G.E.; Chen, D.; Liu, S.X. Physical Properties of Gluten-Free Sugar Cookies Made from Amaranth–Oat Composites. *LWT-Food Sci. Technol.* **2015**, *63*, 214–220. [CrossRef]
28. Barbosa-Cánovas, G.V.; Fontana, A.J.; Schmidt, S.J.; Labuza, T.P. *Water Activity in Foods: Fundamentals and Applications*; John Wiley & Sons: Hoboken, NJ, USA, 2008; pp. 1–435. [CrossRef]
29. BEDCA Base de Datos BEDCA. Available online: https://www.bedca.net/bdpub/ (accessed on 4 June 2023).
30. Fernandes, D.C.; Freitas, J.B.; Czeder, L.P.; Naves, M.M.V. Nutritional Composition and Protein Value of the Baru (*Dipteryx alata* Vog.) Almond from the Brazilian Savanna. *J. Sci. Food Agric.* **2010**, *90*, 1650–1655. [CrossRef]
31. Amagliani, L.; O'Regan, J.; Kelly, A.L.; O'Mahony, J.A. Composition and Protein Profile Analysis of Rice Protein Ingredients. *J. Food Compos. Anal.* **2017**, *59*, 18–26. [CrossRef]
32. Nedeljković, N.; Hadnađev, M.; Dapčević Hadnađev, T.; Šarić, B.; Pezo, L.; Sakač, M.; Pajin, B. Partial Replacement of Fat with Oat and Wheat Bran Gels: Optimization Study Based on Rheological and Textural Properties. *LWT* **2017**, *86*, 377–384. [CrossRef]
33. Lu, F.; Liu, Y.; Li, B. Okara Dietary Fiber and Hypoglycemic Effect of Okara Foods. *Bioact. Carbohydr. Diet. Fibre* **2013**, *2*, 126–132. [CrossRef]
34. Castellanos Fuentes, A.P.; Genevois, C.E.; Flores, S.K.; De Escalada Pla, M.F. Valorisation of Soy By-Products as Substrate for Food Ingredients Containing *L. casei* through Solid State Fermentation. *LWT-Food Sci. Technol.* **2020**, *132*, 109779. [CrossRef]
35. Gul, K.; Yousuf, B.; Singh, A.K.; Singh, P.; Wani, A.A. Rice Bran: Nutritional Values and Its Emerging Potential for Development of Functional Food—A Review. *Bioact. Carbohydr. Diet. Fibre* **2015**, *6*, 24–30. [CrossRef]
36. Hu, M. Chapter 9—Oxidative Stability and Shelf Life of Low-Moisture Foods. In *Oxidative Stability and Shelf Life of Foods Containing Oils and Fats*; Hu, M., Jacobsen, C., Eds.; AOCS Press: Urbana, IL, USA, 2016; pp. 313–371, ISBN 9781630670566. [CrossRef]
37. Guimarães, R.M.; Silva, T.E.; Lemes, A.C.; Boldrin, M.C.F.; da Silva, M.A.P.; Silva, F.G.; Egea, M.B. Okara: A Soybean by-Product as an Alternative to Enrich Vegetable Paste. *LWT* **2018**, *92*, 593–599. [CrossRef]
38. Sánchez-Zapata, E.; Díaz-Vela, J.; Pérez-Chabela, M.L.; Pérez-Alvarez, J.A.; Fernández-López, J. Evaluation of the Effect of Tiger Nut Fibre as a Carrier of Unsaturated Fatty Acids Rich Oil on the Quality of Dry-Cured Sausages. *Food Bioprocess Technol.* **2013**, *6*, 1181–1190. [CrossRef]

39. Chantaro, P.; Devahastin, S.; Chiewchan, N. Production of Antioxidant High Dietary Fiber Powder from Carrot Peels. *LWT-Food Sci. Technol.* **2008**, *41*, 1987–1994. [CrossRef]
40. Elleuch, M.; Bedigian, D.; Roiseux, O.; Besbes, S.; Blecker, C.; Attia, H. Dietary Fibre and Fibre-Rich by-Products of Food Processing: Characterisation, Technological Functionality and Commercial Applications: A Review. *Food Chem.* **2011**, *124*, 411–421. [CrossRef]
41. Jafari, S.M.; Ghalegi Ghalenoei, M.; Dehnad, D. Influence of Spray Drying on Water Solubility Index, Apparent Density, and Anthocyanin Content of Pomegranate Juice Powder. *Powder Technol.* **2017**, *311*, 59–65. [CrossRef]
42. Oliveira, V.M.; Jorge, E.C.; Borges, S.V. Empleo de un Secador por Atomización a Escala Piloto en la Producción de Maracuyá en Polvo y su Aceptabilidad para Elaborar Jugo Reconstituido. *Aliment. Rev. Tecnol. Hig. Aliment.* **2003**, *342*, 83–88.
43. Gay, J.; Campos, F.R.; Oliveira, V.M.; Borges, S.V.; Francisoni, A.D.; Pereira, D.B. Propiedades Físicas del Jugo de Maracuyá en polvo 1: Efecto de la Velocidad de Atomización y Concentración de Maltodextrina. *Aliment. Rev. Tecnol. Hig. Aliment.* **2003**, *346*, 97–100.
44. Bai, X.; Zhang, M.L.; Zhang, Y.; Zhang, J.; Zhang, Y.; Wang, C.; Liu, R. Effects of Steaming, Microwaving, and Hot-Air Drying on the Physicochemical Properties and Storage Stability of Oat Bran. *J. Food Qual.* **2021**, *2021*, 4058645. [CrossRef]
45. Bhusari, S.N.; Muzaffar, K.; Kumar, P. Effect of Carrier Agents on Physical and Microstructural Properties of Spray Dried Tamarind Pulp Powder. *Powder Technol.* **2014**, *266*, 354–364. [CrossRef]
46. Callahan, B.J.; McMurdie, P.J.; Rosen, M.J.; Han, A.W.; Johnson, A.J.A.; Holmes, S.P. DADA2: High-Resolution Sample Inference from Illumina Amplicon Data. *Nat. Methods* **2016**, *13*, 581–583. [CrossRef] [PubMed]
47. Lecumberri, E.; Mateos, R.; Izquierdo-Pulido, M.; Rupérez, P.; Goya, L.; Bravo, L. Dietary Fibre Composition, Antioxidant Capacity and Physico-Chemical Properties of a Fibre-Rich Product from Cocoa (*Theobroma cacao* L.). *Food Chem.* **2007**, *104*, 948–954. [CrossRef]
48. Hinestroza-Córdoba, L.I.; Serna, S.D.; Seguí, L.; Barrera, C.; Betoret, N. Characterization of Powdered Lulo (*Solanum quitoense*) Bagasse as a Functional Food Ingredient. *Foods* **2020**, *9*, 723. [CrossRef]
49. Özdemir, E.E.; Görgüç, A.; Gençdağ, E.; Yılmaz, F.M. Physicochemical, Functional and Emulsifying Properties of Plant Protein Powder from Industrial Sesame Processing Waste as Affected by Spray and Freeze Drying. *LWT* **2022**, *154*, 112646. [CrossRef]
50. Martínez-Las Heras, R.; Landines, E.F.; Heredia, A.; Castelló, M.L.; Andrés, A. Influence of Drying Process and Particle Size of Persimmon Fibre on Its Physicochemical, Antioxidant, Hydration and Emulsifying Properties. *J. Food Sci. Technol.* **2017**, *54*, 2902–2912. [CrossRef]
51. Cheng, F.; Ding, K.; Yin, H.; Tulbek, M.; Chigwedere, C.M.; Ai, Y. Milling and Differential Sieving to Diversify Flour Functionality: A Comparison between Pulses and Cereals. *Food Res. Int.* **2023**, *163*, 112223. [CrossRef]
52. Bodart, M.; de Peñaranda, R.; Deneyer, A.; Flamant, G. Photometry and Colorimetry Characterisation of Materials in Daylighting Evaluation Tools. *Build. Environ.* **2008**, *43*, 2046–2058. [CrossRef]
53. Calabuig-Jiménez, L.; Hinestroza-Córdoba, L.I.; Barrera, C.; Seguí, L.; Betoret, N. Effects of Processing and Storage Conditions on Functional Properties of Powdered Blueberry Pomace. *Sustainability* **2022**, *14*, 1839. [CrossRef]
54. Saez, R. Caracterización de Polvos de Piel de Mandarina para su Uso como Ingrediente Funcional en Alimentos. Available online: https://www.google.com.hk/url?sa=t&rct=j&q=&esrc=s&source=web&cd=&cad=rja&uact=8&ved=2ahUKEwiKzbzB0Pv_AhXimFYBHaoRDhMQFnoECAsQAQ&url=https%3A%2F%2Friunet.upv.es%2Fbitstream%2Fhandle%2F10251%2F93422%2FS%25C3%2581EZ%2520-%2520CARACTERIZACI%25C3%2593N%2520DE%2520POLVOS%2520DE%2520PIEL%2520DE%2520MANDARINA%2520PARA%2520SU%2520USO%2520COMO%2520INGREDIENTE%2520FUNCIONAL%2520EN%2520A....pdf%3Fsequence%3D1&usg=AOvVaw02o4F1-7vzzC40ZjullLzV&opi=89978449 (accessed on 20 January 2023).
55. Bas-Bellver, C.; Andrés, C.; Seguí, L.; Barrera, C.; Jiménez-Hernández, N.; Artacho, A.; Betoret, N.; Gosalbes, M.J. Valorization of Persimmon and Blueberry Byproducts to Obtain Functional Powders: In Vitro Digestion and Fermentation by Gut Microbiota. *J. Agric. Food Chem.* **2020**, *68*, 8080–8090. [CrossRef] [PubMed]
56. Garrido, I.; Monagas, M.; Gómez-Cordovés, C.; Bartolomé, B. Extracción de Antioxidantes a Partir de Subproductos del Procesado de la Almendra. *Grasas Aceites* **2007**, *58*, 130–135. [CrossRef]
57. Bolling, B.W.; Chen, C.Y.O.; McKay, D.L.; Blumberg, J.B. Tree Nut Phytochemicals: Composition, Antioxidant Capacity, Bioactivity, Impact Factors. A Systematic Review of Almonds, Brazils, Cashews, Hazelnuts, Macadamias, Pecans, Pine Nuts, Pistachios and Walnuts. *Nutr. Res. Rev.* **2011**, *24*, 244–275. [CrossRef]
58. Ribarova, F.; Marinova, D.; Ribarova, F.; Atanassova, M. Total Phenolics and Flavonoids in Bulgarian Fruits and Vegetables. *J. Univ. Chem. Technol. Metall.* **2005**, *40*, 255–260.
59. Kornsteiner, M.; Wagner, K.H.; Elmadfa, I. Tocopherols and Total Phenolics in 10 Different Nut Types. *Food Chem.* **2006**, *98*, 381–387. [CrossRef]
60. Inyang, U.E.; Oboh, I.O.; Etuk, B.R.; Inyang, U.E.; Oboh, I.O.; Etuk, B.R. Kinetic Models for Drying Techniques—Food Materials. *Adv. Chem. Eng. Sci.* **2018**, *8*, 27–48. [CrossRef]
61. Ling, W.; Xing, Y.; Hong, C.; Zhang, B.; Hu, J.; Zhao, C.; Wang, Y.; Feng, L. Methods, Mechanisms, Models and Tail Gas Emissions of Convective Drying in Sludge: A Review. *Sci. Total Environ.* **2022**, *845*, 157376. [CrossRef]
62. Srikiatden, J.; Roberts, J.S. Moisture Transfer in Solid Food Materials: A Review of Mechanisms, Models, and Measurements. *Int. J. Food Prop.* **2007**, *10*, 739–777. [CrossRef]

63. Onwude, D.I.; Hashim, N.; Janius, R.B.; Nawi, N.M.; Abdan, K. Modeling the Thin-Layer Drying of Fruits and Vegetables: A Review. *Compr. Rev. Food Sci. Food Saf.* **2016**, *15*, 599–618. [CrossRef] [PubMed]
64. Maskan, A.; Kaya, S.; Maskan, M. Hot Air and Sun Drying of Grape Leather (Pestil). *J. Food Eng.* **2002**, *54*, 81–88. [CrossRef]
65. Aghbashlo, M.; Kianmehr, M.H.; Samimi-Akhijahani, H. Influence of Drying Conditions on the Effective Moisture Diffusivity, Energy of Activation and Energy Consumption during the Thin-Layer Drying of Berberis Fruit (Berberidaceae). *Energy Convers. Manag.* **2008**, *49*, 2865–2871. [CrossRef]
66. Saravacos, G.D.; Maroulis, Z.B. *Transport Properties of Foods*; CRC Press: Boca Raton, FL, USA, 2001. [CrossRef]
67. Xiong, X.; Narsimhan, G.; Okos, M.R. Effect of Composition and Pore Structure on Binding Energy and Effective Diffusivity of Moisture in Porous Food. *J. Food Eng.* **1992**, *15*, 187–208. [CrossRef]
68. Zhao, G.; Yin, F.; Liang, X.; Yuan, D.; Geng, W.; Wang, L.; Sun, R. Drying Experiment and Drying Model Analysis of Dehydrated Sludge Particles. *IOP Conf. Ser. Mater. Sci. Eng.* **2020**, *768*, 022031. [CrossRef]
69. Labuza, T.P.; Kaanane, A.; Chen, J.Y. Effect of Temperature on the Moisture Sorption Isotherms and Water Activity Shift of Two Dehydrated Foods. *J. Food Sci.* **1985**, *50*, 385–392. [CrossRef]
70. Pahlevanzadeh, H.; Yazdani, M. Moisture adsorption isotherms and isosteric energy for almond. *J. Food Process Eng.* **2005**, *28*, 331–345. [CrossRef]
71. See, X.Y.; Dupas-Langlet, M.; Forny, L.; Meunier, V.; Zhou, W. Physical Stability of Co-Freeze-Dried Powders Made from NaCl and Maltodextrins—Impact of NaCl on Glass Transition Temperature, Water Vapour Sorption Isotherm and Water Vapour Sorption Kinetics. *Food Hydrocoll.* **2023**, *136*, 108238. [CrossRef]